ISSN 1063-7788, Physics of Atomic Nuclei, 2017, Vol. 80, No. 11, pp. 1683–1686. © Pleiades Publishing, Ltd., 2017.
Original Russian Text © V.V. Kuzenov, 2016, published in Yadernaya Fizika i Inzhiniring, 2016, Vol. 7, No. 4, pp. 342–346.

GAS DISCHARGE AND PLASMA PHYSICS

Computer Simulation of Compression and Energy Release upon Laser Irradiation of Cylindrically Symmetric Target

V. V. Kuzenov[a,b]

[a] Bauman Moscow State Technical University (National Research University), Moscow, Russia
[b] Dukhov All-Russia Research Institute of Automatics, Moscow, Russia
e-mail: vik.kuzenov@gmail.com

Received October 31, 2016

Abstract—The paper is devoted to the theoretical and computational study of compression and energy release for magneto-inertial plasma confinement. This approach makes it possible to create new high-density plasma sources, apply them in materials science experiments, and use them in promising areas of power engineering.

Keywords: high energy density, laser beams, magneto-inertial fusion, mathematical modeling, cylindrical target

DOI: 10.1134/S1063778817090101

INTRODUCTION

Recently, experimental and theoretical studies [1–5] of the magneto-inertial plasma confinement method or magneto-inertial fusion (MIF), which is based on a combination of external plasma heating sources (drivers, i.e., laser beams or supersonic plasma jets) and a seed magnetic field, have been notably developed. Under this approach, it is of fundamental importance to have a seed magnetic field that is amplified by laser target compression and prevents electron heat transfer, which takes energy from the central heated part, and that can hold almost all the emitted fast charged particles, which after several nuclear scattering events expend their energy on heating of the adjacent plasma regions.

Note that in [4] the authors provided initial estimates of the thermophysical plasma parameters and of the energy costs of the electromagnetic field compression and eddy currents.

In this paper, the compression and heating of a magnetized cylindrically symmetric target exposed to the laser driver are computer simulated [6–8].

FORMULATION OF PROBLEM AND NUMERICAL METHOD FOR CALCULATING PLASMA PARAMETERS

A mathematical model describing the physical processes in a cylindrically symmetric MIF target is given in [4, 9, 10] and is based on one-dimensional equations of radiation plasmodynamics: the system of Euler equations; the transfer equation for intrinsic broadband radiation, the magnetic induction equation; the laser radiation transfer equation; methods for calculating the equations of state of matter and the absorption coefficients of laser radiation, which determine the conditions for the onset and flow of a self-sustaining fusion reaction.

The region of computation and the MIF target consist of the central part and one coaxial layer. They are cylindrically shaped with the following range of values of the initial parameters of the target and the medium:

The central part of the target (radius of the nucleus $R_n = 0.05$ cm) is filled with a D–T mixture with a density of $\rho = 5 \times 10^{-2}$ g/cm^3 and an initial temperature of $T = 297$ K. It is surrounded by a coaxial layer (with an outer radius of $R_c = 0.1$ cm) consisting of metal (Al) with a density of $\rho = 2.7$ g/cm^3 and an initial temperature of $T = 297$ K.

The region of computation has an outer radius of $l = 0.2$ cm. Thermodynamic parameters of the external rarefied medium (consisting of Ar) are given by the values $T = 297$ K and $\rho = 2.7 \times 10^{-3}$ g/cm^3.

Initial values of the strength of the seed magnetic field in a rarefied medium are the fractions of a tesla. The spectral flux and the bulk density of broadband radiation and the laser flux for $r \in [0, \ell]$ at the initial time $t = 0$ are zero.

Despite the one-dimensional nature of the considered problem, it imposes serious requirements on the numerical method used to solve it:

The computational model should have improved dispersive and dissipative properties, be energy efficient, have the property of monotonicity, and approximate smooth solutions preferably with the highest possible accuracy.

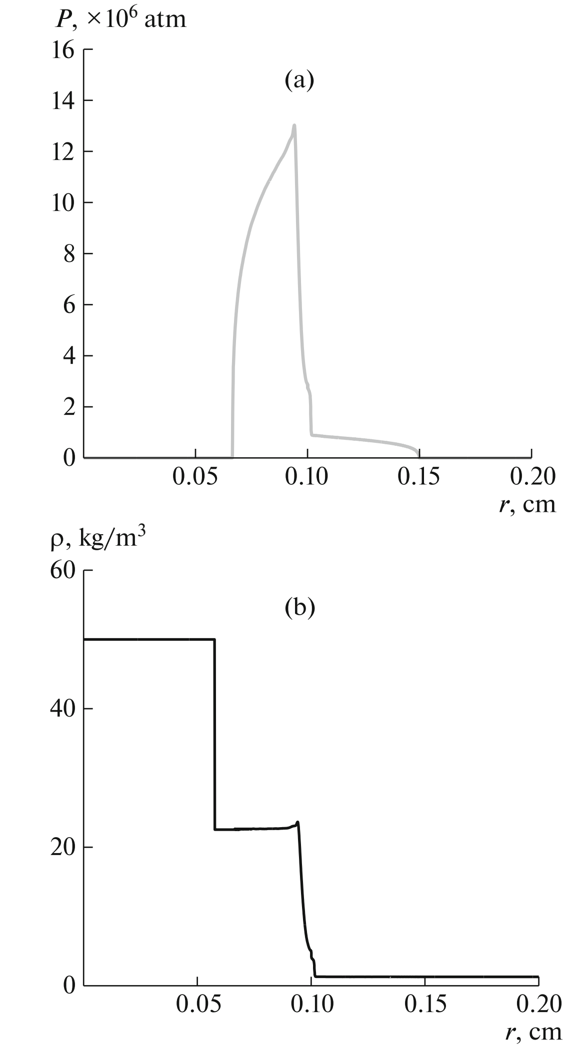

Fig. 1. Spatial distribution of pressure (a) and density (b) at the time $t = 0.19$ ns.

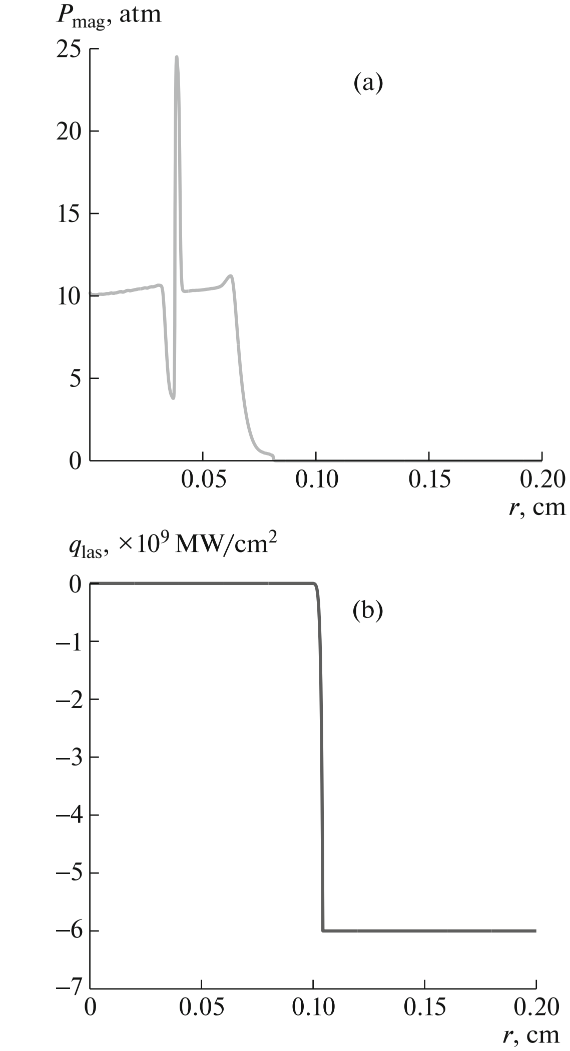

Fig. 2. Spatial distribution of magnetic pressure (a) and laser flux (b) at the time $t = 0.19$ ns.

These requirements are satisfied by the numerical method developed and described in [4, 9, 10]. Note that this numerical method allows computer simulation of all the basic physical patterns inherent in MIF.

INDIVIDUAL COMPUTATIONAL RESULTS

The convective and thermal parts of the computer target model were tested in studies of the authors [9, 10].

The group of calculations carried out in the paper with a radiation flux density at the level of $q_{\text{las}} \approx 1 \times 10^{12}–1 \times 10^{14}$ W/cm^2 showed that the laser compression of a target located in an external magnetic field with respect to the time t can be conventionally represented in the form of three stages:

• Initial compression stage of the magnetized target.

• Collapse stage of the plasma target.

• Spread stage of plasma formation.

Next, let us provide a brief description of the results obtained for the laser flux density $q_{\text{las}} = 6 \times 10^{15}$ W/cm^2.

Figures 1–4 show the distributions of static pressure P and magnetic pressure P_{mag}, density ρ and temperature T, and flux of total q and laser q_{las} radiation corresponding to the stages of compression of targets for the MIF and the following parameters of the mathematical model:

• Local (thermonuclear) energy release $Q^e_{\text{Fus}} \neq 0$ into the electronic component of the plasma.

• Flux density of laser radiation $q_{\text{las}} = 6 \times 10^{15}$ W/cm^2, half-width of the laser pulse $\tau = 10$ ns.

Figures 1 and 2 show the distributions of the static P and magnetic P_{mag} pressure, the density ρ, and the laser flux q_{las} which correspond to the first initial stage

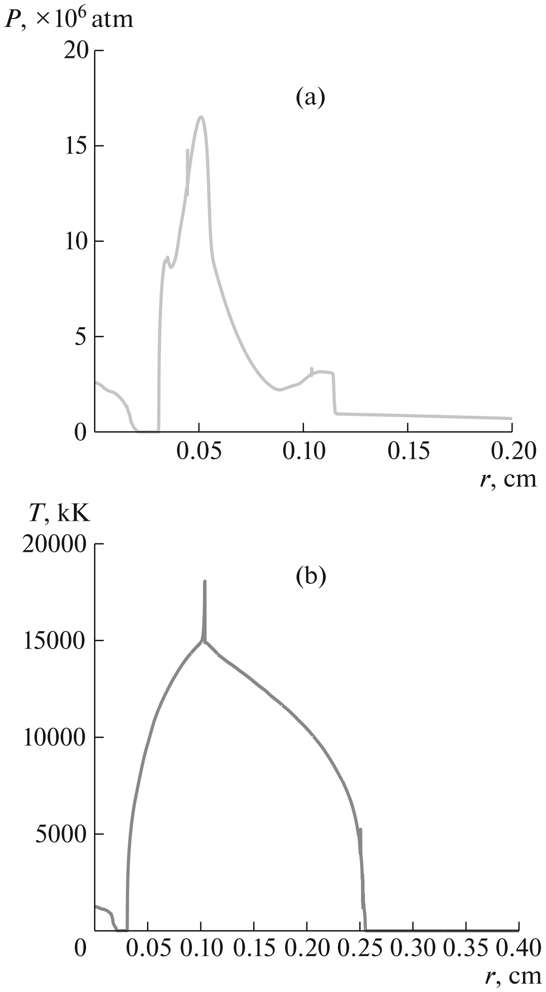

Fig. 3. Spatial distribution of pressure (a) and temperature (b) at the time $t = 0.38$ ns.

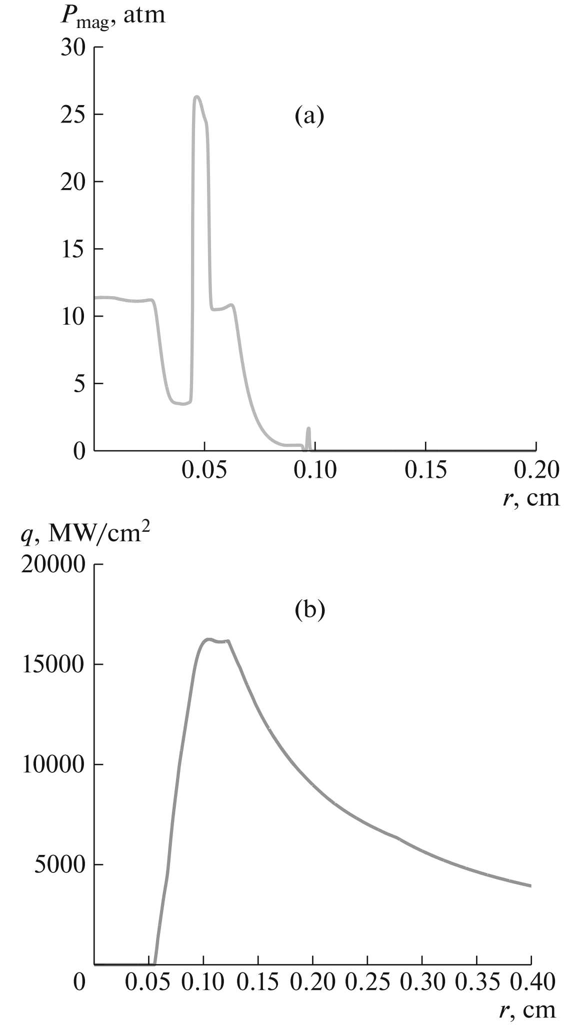

Fig. 4. Spatial distribution of magnetic pressure (a) and the total flux of the intrinsic radiation of the plasma (b) at the time $t = 0.593$ ns.

($t = 0.19$ ns) of the MIF target compression located in an external magnetic field.

Graphical dependences shown in Fig. 3 correspond to the collapse stage of the magnetized target.

Figure 4 shows the distributions of the magnetic pressure P_{mag} and the total flux q of the intrinsic radiation of the plasma formation corresponding to the spread stage of the plasma formation ($t = 0.593$ ns).

CONCLUSIONS

One-dimensional mathematical models and numerical methods of increased accuracy have been developed [11–14] that make it possible to compute compression and heating of MIF targets in an external magnetic field for a centrally symmetric coordinate system. Initial calculations of all the main gas-dynamic and radiative parameters of the laser plasma of the target were carried out. Numerical simulation of the compression of the target (for $q_{\text{las}} = 1\times10^{12}$–$6\times10^{15}$ W/cm^2 consisting of the central part and one coaxial layer showed the following:

During compression, the central part of the target is optically transparent both to laser radiation and to the intrinsic broadband plasma radiation. However, the density of heat fluxes on the first wall of the reactor chamber at certain instants can reach ~10^{11} W/cm^2.

During MIF target compression, the level of magnetic pressure P_{mag} in the plasma varies with time and is comparable to the static pressure P (reaching the values of ~10^6 atm).

The maximum values of the pressure and temperature of the target plasma are observed at the time 0.2–5 ns after the shock wave reflects from the geometric axis of symmetry.

It can also be noted that the MIF target plasma is a powerful source of magnetic flux and broadband radiation that increases in time (at the first and second stages). All this allows us to hope that the MIF-based approach is suitable for the creation of new plasma sources of intense broadband radiation and fluxes of high-density particles and their application in materials science experiments and in promising areas of power engineering.

ACKNOWLEDGMENTS

This work was supported by the Ministry of Education and Science of the Russian Federation, project no. 13.5240.2017/8.9.

REFERENCES

1. M. L. Shmatov, Phys. At. Nucl. **79**, 666 (2016).
2. I. Yu. Kostyukov and S. V. Ryzhkov, Plasma Phys. Rep. **37**, 1092 (2011).
3. A. S. Boldarev, E. A. Bolkhovitinov, I. Yu. Vichev, G. S. Volkov, V. A. Gasilov, et al., Plasma Phys. Rep. **41**, 178 (2015).
4. V. V. Kuzenov and S. V. Ryzhkov, Vopr. At. Nauki Tekh., Ser.: Fiz. Plasmy, No. 1 (83), 12 (2013).
5. V. V. Shumaev, Phys. At. Nucl. **79**, 1414 (2016).
6. V. P. Krainov, Phys. At. Nucl. **74**, 1410 (2011).
7. S. V. Ryzhkov, Vopr. At. Nauki Tekh., Ser.: Plazm. Elektron. Nov. Metody Uskoren., No. 4 (68), 105 (2010).
8. V. V. Kuzenov and S. V. Ryzhkov, Vopr. At. Nauki Tekh., Ser.: Plazm. Elektron. Nov. Metody Uskoren., No. 4 (86), 103 (2013).
9. V. V. Kuzenov and S. V. Ryzhkov, Bull. Russ. Acad. Sci.: Phys. **80**, 598 (2016).
10. V. V. Kuzenov and S. V. Ryzhkov, Mat. Model. **29**, 19 (2017); Math. Models Comput. Simul. **10** (2018, in press).
11. V. V. Kuzenov and S. V. Ryzhkov, J. Phys.: Conf. Ser. **830**, 012124 (2017).
12. V. V. Kuzenov and S. V. Ryzhkov, Appl. Phys. **3**, 26 (2014).
13. V. V. Kuzenov, A. I. Lebo, I. G. Lebo, and S. V. Ryzhkov, *Physico-Mathematical Models and Methods for Calculating the Effect of High-Power Laser and Plasma Pulses on Condensed and Gaseous Media* (Bauman Mosk. Gos. Tekh. Univ., Moscow, 2015) [in Russian].
14. S. V. Ryzhkov, Sustain. Cities Soc. **14**, 313 (2015).

Translated by O. Pismenov